GEOSPHERE

GEOSPHERE, v. 15, no. 2

https://doi.org/10.1130/GES01657.1

14 figures; 1 set of supplemental files

CORRESPONDENCE: rhuene@mindspring.com

CITATION: von Huene, R., Miller, J.J., and Krabbenhoeft, A., 2019, The Shumagin seismic gap structure and associated tsunami hazards, Alaska convergent margin: Geosphere, v. 15, no. 2, p. 324–341, https://doi.org/10.1130/GES01657.1.

Science Editor: Shanaka de Silva
Associate Editor: Laura M. Wallace

Received 29 December 2017
Revision received 23 October 2018
Accepted 28 December 2018

Published online 29 January 2019

The Shumagin seismic gap structure and associated tsunami hazards, Alaska convergent margin

Roland von Huene[1,*,†], John J. Miller[2,*,†], and Anne Krabbenhoeft[3]

[1]U.S. Geological Survey, 800 Blossom Hill Road, Los Gatos, California 95032, USA
[2]U.S. Geological Survey, Denver Federal Center, Denver, Colorado 80225, USA
[3]GEOMAR Helmholz Centre for Ocean Research, D-24148, Kiel, Germany

ABSTRACT

The potential for a major earthquake in the Shumagin seismic gap, and the tsunami it could generate, was reported in 1971. However, while potentially tsunamigenic splay faults in the adjacent Unimak and Semidi earthquake segments are known, such features along the Shumagin segment were undocumented until recently. To investigate margin structure and search for splay faults, we reprocessed six legacy seismic records and also processed seismic data acquired by RV *Langseth* during the ALEUT project (cf. Bécel et al., 2017). All records show splay faults separating the frontal prism from the margin framework. A ridge uplifted by the splay fault hanging wall extends along the entire segment. At the plate interface, the splay fault cuts across subducted sediment strata in some images, whereas in others, the plate interface sediment cuts across the fault. Splay fault zones are commonly associated with subducting lower-plate relief.

Along the upper slope, beneath a sediment cover, major normal faults dipping landward and seaward border a ridge of basement rock. The faults displace a regional unconformity that elsewhere received Oligocene–Miocene sediment. Low seafloor scarps above some normal faults indicate recent tectonism. The buried ridge is a continuation of the Unimak Ridge structure that extends NE of the Unimak/Shumagin segment boundary. Some geological characteristics of the Shumagin segment differ from those of other Alaskan earthquake segments, but a causal link to the proposed Shumagin creeping seismic behavior is equivocal.

INTRODUCTION

Background

Along the Alaska convergent margin, three of four earthquake rupture zones represent areas where aftershocks occurred following great instrumentally recorded earthquakes. From NE to SW, these are the Kodiak segment that ruptured in the 1964 great earthquake, the Semidi segment that broke in a 1938 earthquake, and the Unimak segment that ruptured in 1946. In contrast, the Shumagin segment has no historic great earthquake and is constrained by its neighboring segments rather than its own aftershocks. Since Sykes (1971) first drew attention to the Shumagin segment, it has been a proposed seismic gap. Earthquakes in the adjacent segments have produced tsunamis. To the southwest, during the 1946 M8.6 earthquake, the Unimak segment generated the largest Alaskan tsunami ever recorded in the era of instrumental seismology. This earthquake featured low rupture velocities, a long duration, and a lack of high frequency radiation. It was the first recognized tsunami earthquake in that it produced an outsized tsunami wave compared to its moment magnitude (Kanamori, 1972). Northeast of the Shumagin segment is the Semidi segment, which ruptured in the 1938 M8.2 earthquake and produced only a small tsunami because of the rupture's great depth. Geodetic studies indicate the Semidi segment is currently locked (Fournier and Freymueller, 2007). Meanwhile, geodetic studies in the intervening Shumagin segment have failed to show a stress buildup, and to explain these observations, Fournier and Freymueller (2007) proposed that this segment is creeping rather than releasing stress in large earthquakes. The Shumagin segment's behavior is inconsistent with the rest of the Alaska-Aleutian subduction zone, but this phenomenon has not been investigated with comprehensive geologic analyses since the reports of Bruns et al. (1987) and Lewis et al. (1988).

The Shumagin earthquake rupture segment extends northeastward from Sanak Island to a short distance past the Shumagin Islands (Fig. 1). We reprocessed legacy seismic data acquired by the U.S. Geological Survey (USGS) vessel Lee in 1981 and 1982 (L8-81-WG and L12-82-WG), which were reported in a comprehensive initial marine geological study (Bruns et al., 1987). Additional data from a 1994 transect by RV *Ewing* (EW9409) were reprocessed as well (Miller et al., 2014). We also processed data along three lines acquired during the ALEUT project cruise of RV *Langseth* in 2011 (MGL1110); these data were reported recently with a focus on the plate interface (Li et al., 2015; Bécel et al., 2017; Li et al., 2018). Here, we focus on the tectonics and extent of an out-of-sequence or splay fault along the lower slope and an extensional fault zone along the upper slope. The splay fault is a continuation of a structure in the adjacent Unimak segment (Miller et al., 2014; von Huene et al., 2014)

*Emeritus
†E-mail: rhuene@mindspring.com; jmiller@usgs.gov

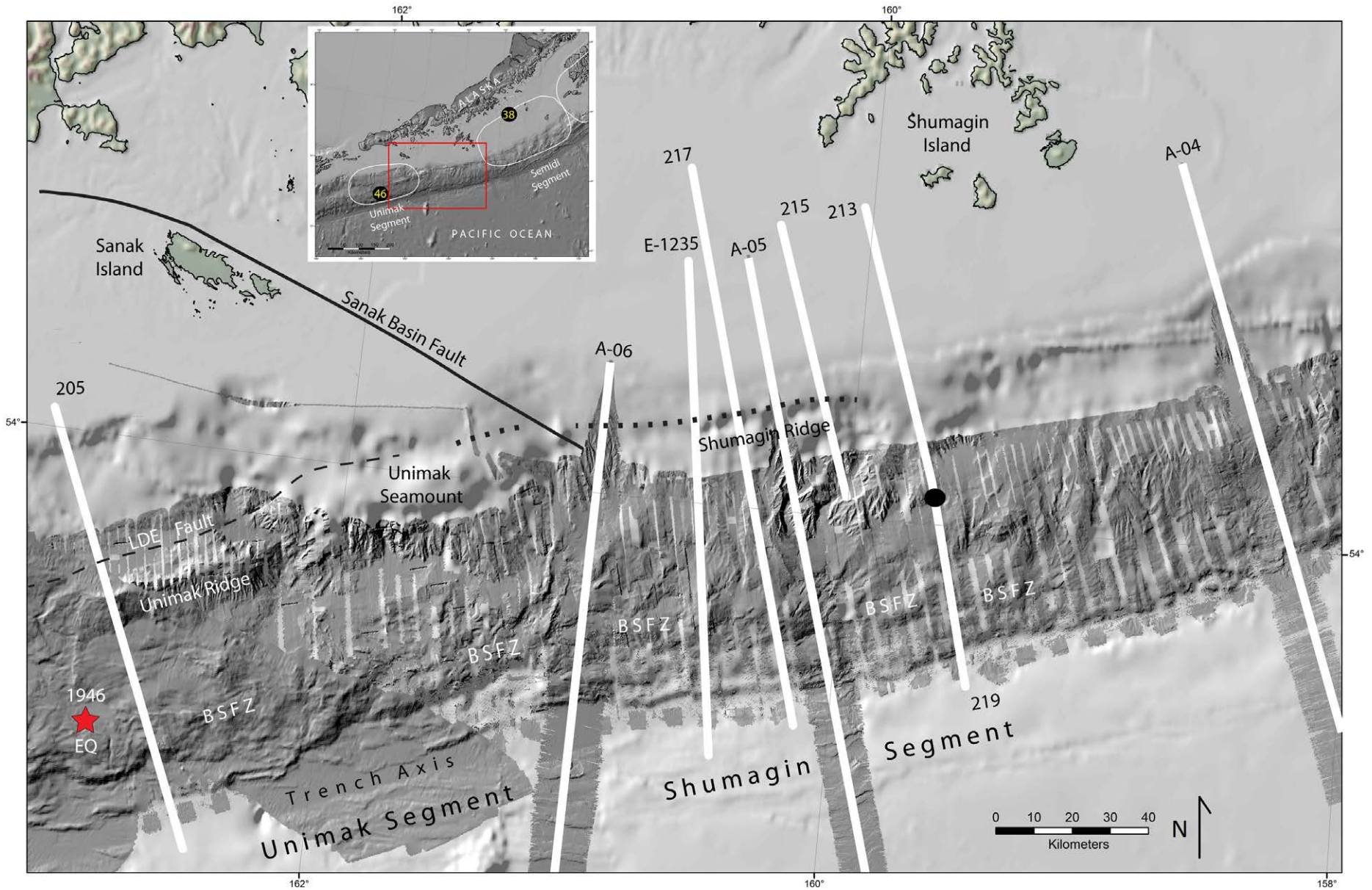

Figure 1. Location of seismic lines in the Shumagin region plotted on the bathymetric compilation of Lim et al. (2009), which includes the survey of Lewis et al. (1988) and in the SW, multibeam data in von Huene et al. (2016). Darkened areas are the multibeam bathymetry. Reprocessed legacy seismic lines are numbered as in Miller et al. (2014) and are without a letter designation; a Ewing line is prefaced with E, and ALEUT lines with A. Line 213, was completed with line 219. In the inset map, earthquake segments with epicenter and year in black dot are outlined in yellow. BSFZ—the backstop splay fault zone; LDE—landward dipping extensional fault, dashed at the base of the upslope-facing seafloor scarp and dotted where completely buried; red star—1946 Unimak earthquake epicenter. U.S. Geological Survey data were acquired in 1982 on cruise L-12-82 -WG: Ewing data in 1995 on EW9409 and ALEUT data on RV *Langseth* in 2011 on cruise MGL1110.

SUPPLEMENTAL DATA

Seismic processing sequence

Reprocessing included trace editing, multiple suppression, deconvolution, velocity analysis, scaling, post-stack migration, and for some lines, pre-stack depth migration (Figs S 1 and S 2). Deconvolution increased the temporal resolution, and migration improved structural detail by properly positioning the reflectors in space, thereby collapsing diffractions to their point of origin. This reprocessing resolved fault plane reflections that in the past were only inferred from stratal truncations (Fig S1). The resulting images resolve previously undetected tectonic relations in the frontal prism backstop area and structures in the zone of extensional faulting. We found that the resolution of post-stack time migrated images converted to depth was commonly similar to that of pre-stack depth migrated images. Depth conversion with interval velocities from stacking was applied to shallow strata, and velocities in deep regions were guided by a wide-angle crustal velocity section in the Unimak segment [Lizarralde et al., 2002]. Reprocessing achieved imaging to greater depth, especially in lines where enhanced multiple rejection was applied. We used a similar processing sequence for Aleut lines 04, 05, and 06, and the superior acquisition parameters (12.5 m versus 24 m trace interval, 8 km versus 2.4 km streamer length, and a larger seismic source) afforded greater resolution (Fig S1 c).

Extensional fault across the upper plate

The remarkable LDE fault zone image developed with ALEUT line 05 data [Bécel et al., 2017] shows that the LDE fault can be rooted in the plate interface. This is indeedan amazing image since the velocity contrast that produces a reflection across a dipping fault zone is normally too small to produce a readable image at 20 to 40 km depth. The LDE fault zone bright spot reflections appear to be 1 to 2 km thick and discontinuous, whereas those from the plate interface are thin and continuous. Dipping reflections from such great depths require an impedance contrast such as that caused by a large concentration of fluid. It may be that they exist locally, which could explain why similar features are not seen in the 6 other RV Langseth lines that cross the Alaska convergent margin.

[1]Supplemental Information. Seismic image improvement from updated seismic processing and the Shumagin margin morphology in perspective views. Please visit https://doi.org/10.1130/GES01657.S1 or access the full-text article on www.gsapubs.org to view the Supplemental Information.

and similar to a splay fault in the Semidi segment (von Huene et al., 2016). A landward-dipping extensional (LDE) fault zone (Bécel et al., 2017) is an element of the upper-slope extensional zone. The fault's imaged extent to the plate interface is extraordinary. It occurs along an upper-slope ridge that appears to continue SW as Unimak Ridge.

The Shumagin segment's SW boundary with the Unimak segment corresponds with a major upper-plate tectonic unit. It contains two tectonic features atypical of the Alaska margin, namely the diagonal NW-trending Sanak Basin and the Unimak Seamount (Fig. 1) (Bruns et al., 1987). It is discussed in more detail below. The NE boundary with the Semidi segment is apparent from bathymetry, but with little seismic data, the underlying boundary structures are unknown.

In our study, we apply current seismic processing software to legacy data, with a focus on two structures associated with potential tsunami generation in the Shumagin segment (Supplemental Figs. S1 and S2[1]). Integration of bathymetric data with seismic-reflection data shows the extent of the splay fault zone along the lower slope (Fig. 1). With more seismic images and enhanced resolution, we show the extent and character of the splay fault identified in ALEUT line 6 (Bécel et al., 2017). Higher up on the margin, the zone of extensional deformation across the foot of the upper slope reveals structural features that are commonly obscured at the upper- to mid-slope juncture in other Alaskan margins seismic images.

The Backstop Splay Fault Zone Concept

Tsunami hazards due to faults that branch from the plate interface and follow a path behind the frontal prism were first appreciated in studies of the Nankai convergent margin (cf. Moore et al., 2007). In Nankai, the frontal prism is separated from an older rock mass by a seaward-verging thrust fault zone termed a splay fault (Moore et al., 2007). The fault zone provides a shortened path for slip propagation from the seismogenic zone to the lower-slope seafloor compared to the plate interface path toward the trench axis. Because the splay's dip is steeper and its path shorter than the plate interface path, a given amount of slip results in greater seafloor uplift (Wendt et al., 2009). To retain the original sense of the Nankai margin fault zone and separate it from thrust faults termed splays on the Alaskan shelf (cf. Liberty et al., 2013), we termed these splays "backstop splay fault zones" (BSFZs). They occur in very deep water (>3 km), and thus they can generate much larger tsunamis than thrust faults on the shelf. Since BSFZ is a new term, we explain before proceeding to an explanation of data.

Backstop is a term often applied to a lower-slope area where stratal reflections lose coherence and image reflectivity is scattered. This term is commonly assumed to indicate consolidated complexly deformed accretionary strata that have also lost impedance contrasts. Here we show that along the Alaska margin, the backstop is a transition from the seaward end of the margin framework to the landward end of the frontal prism. Framework rock corresponds with the acoustic basement that is unconformably overlain by a stratified cover. In all Alaskan earthquake segments, this unconformity returns a characteristic high-amplitude reflection. That reflection extends from the shelf downslope. In transects with less deformed middle slopes, it is imaged to the backstop area. On the Shumagin shelf, the unconformity can be traced from the insular subaerial outcrops across the shelf and down into the mid-slope area (Bruns et al., 1987; their figure 8, horizon A). Here, wide-angle seismic data generally indicate an acoustic basement velocity greater than 4.6 km/s (Bruns et al., 1987), and 19 Sonobuoy records give an average velocity contrast across the unconformity of 2 km/s. This explains the robust reflectivity that makes it a geologic marker. The diffuse reflectivity of basement is different from the deformed strata of the frontal prism; so the transition from one to the other can be recognized from reflective character *when seismic resolution allows*.

The frontal prism is characterized by deformed stratal reflections. Seismic images of trench axis strata merge into an imbricated frontal prism that extends up slope to a lower or middle-slope seafloor juncture. That juncture is marked by a landward-dipping zone of short and diffuse landward-dipping reflections and is commonly a complexly structured transition between the frontal prism and margin framework basement. On the landward side is a disrupted down-slope end of the Oligo-Miocene unconformity. The unconformity reflection can be traced to the backstop area in several Alaskan margin seismic images (Fig. 2). It is assumed that the unconformity on acoustic basement is also the top of continental basement rock. This is not peculiar to the Alaskan margin since shallow-water sediment was recovered from the lower slope of the Peru and Central American margins.

The acoustic basement unconformity is also an inferred time horizon. Beneath the shelf, framework basement is correlated with the Cretaceous Shumagin Formation, named for offshore insular outcrops along the Alaska Peninsula (Burk, 1965; Moore, 1972). The Shumagin Formation is part of an extensive regional belt of similar Cretaceous metamorphic rock studied most extensively along the Kodiak Islands shelf. There Cretaceous basement is overlain unconformably by Eocene to Recent strata, dated in dredged and drilled sections (Winston, 1983; Turner et al., 1987; von Huene et al., 1987). Oligocene rock that is 1500 m thick on shore is missing in three of four industry exploratory drill holes, indicating a period of profound erosion. The unconformity is probably a time-transgressive temporal marker reflection. Following Bruns et al. (1987), we refer to it as the Oligocene/Miocene unconformity, recognizing a period of time to the youngest sampled age of sediment deposited upon it (Turner et al., 1987).

GEOPHYSICAL DATA

BSFZ Bathymetry

In regional bathymetric maps of the Shumagin segment, a BSFZ ridge like that of adjacent segments extends from the Unimak segment to the Shumagin Islands that then diminishes to become almost imperceptible near the Semidi segment (Figs. 1 and S3 and S4 [footnote 1]). GLORIA sidescan images (https://

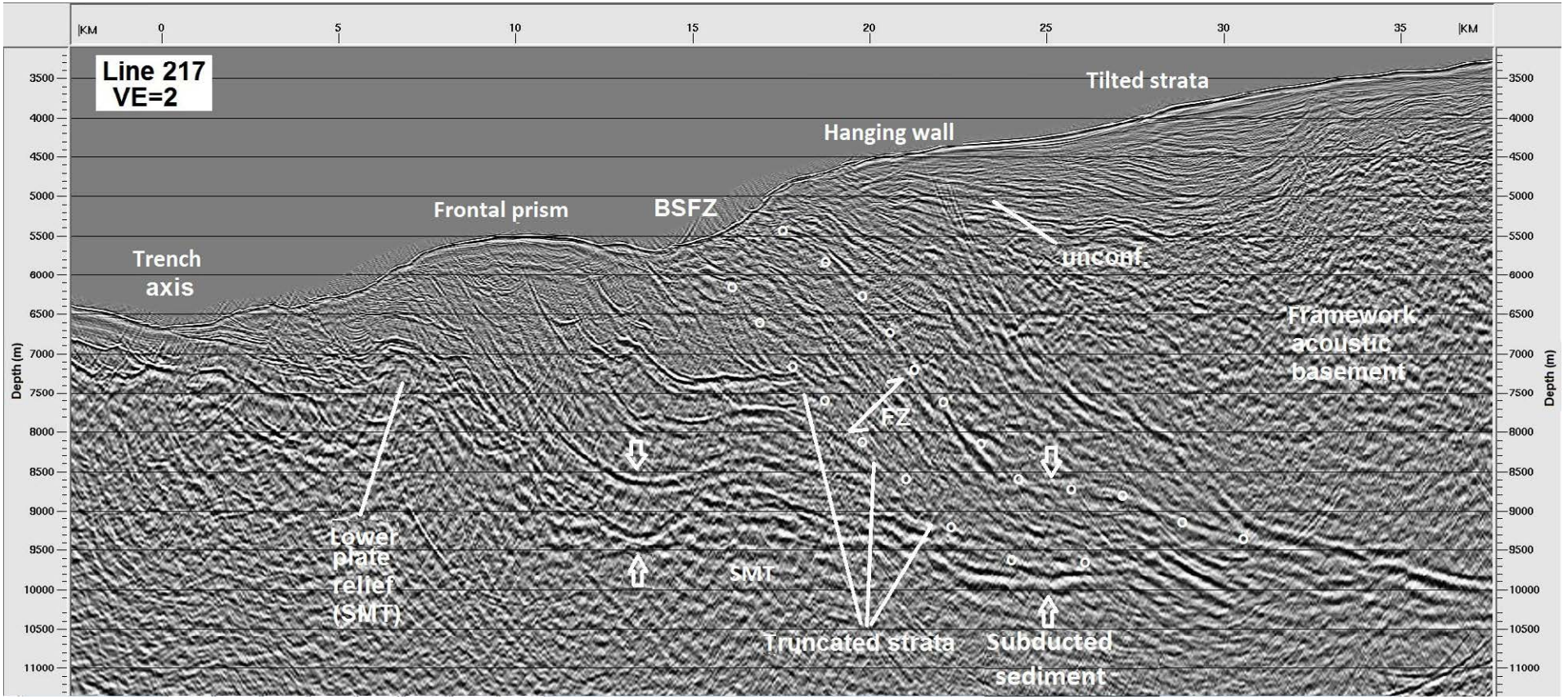

Figure 2. Migrated depth section of legacy line 217. Dots lead the eye along the backstop splay fault zone (BSFZ) edges interpreted from truncated strata of the frontal prism and truncated reflectivity of the margin framework. The BSFZ also has local continuous strong reflections. Disrupted reflectivity is interpreted as a damage zone (FZ). It crosses not only frontal prism strata but also some of the subducted sediment layer (opposing arrows). Because lower-plate relief ~1 km high beneath the frontal prism has been resolved, the continuity of the plate interface appears interrupted. SMT—seamount or other lower-plate relief. The hanging wall consists of acoustic basement that is capped by landward tilted strata in a slope basin. Unconformity (unconf.) covered with sediment of inferred Oligocene–Miocene age. The image clarity is improved with enlargement. VE—vertical exaggeration.

pubs.usgs.gov/of/2010/1332/htmldocs/gak/gak_indexmap.html) are consistent with bathymetry, resolving irregular peaks and saddles along the BSFZ ridge, with local sharp outcrops of erosion-resistant beds (Paskevich et al., 2010). Where seismic lines cross a peak, they show a sudden steep slope, while the slope remains almost unchanged across saddles. The BSFZ ridge is 6–7 km wide and 10–14 km from the deformation front. Slope failure scars and mass-wasting deposits are numerous.

A decreasing height and roughness of seafloor features characterize the morphology between line 213/219 and ALEUT 04 (Fig. 1). Northeast of ALEUT 04, the smoother morphology is cut by deep canyons in a transition to the characteristic morphology of the Semidi segment.

BFSZ Seismic Images

Legacy seismic images in Bruns et al. (1987) were processed with 1980s software. Our reprocessing with current software included trace editing, multiple suppression, deconvolution, velocity analysis, scaling, post-stack migration, and for some lines, pre-stack depth migration (Figs. S1 and S2 [footnote 1]). Processing is further described in the Supplemental Information (footnote 1).

Five seismic images across the BSFZ are concentrated in the SW half of the Shumagin segment (Fig. 1). ALEUT 06 crosses a morphological notch along the boundary between the Unimak and Shumagin segments. Bécel et al. (2017) took note of a BSFZ in ALEUT 06 and mentioned its tsunami potential. At the

NE boundary, line ALEUT 04 is in a transition to the Semidi segment (Fig. 1). The SW group of five images illustrates the amount of structural variability along strike (Figs. 2–6 and S3 and S4 [footnote 1]).

We begin with legacy line 217 (Fig. 2), which shows a basic structure with greater clarity than in other images. At the frontal prism landward limit, the BSFZ cuts the flank of strata arched over subducted lower-plate relief. These truncated frontal prism strata and those on the opposite side along the margin framework are interpreted as the limits of the BSFZ fault damage zone. The 8.5–9.5 km depth of the connection between the BSFZ and the plate interface is relatively shallow. This facilitates seismic resolution of this critical junction, owing to shortened acoustic travel paths and the absence of a seafloor multiple. The BSFZ reflectivity (Fig. 2) continues through the junction with the plate interface subducted sediment cutting off the megathrust sector beneath the frontal prism. It can become a principal source of fragmented fault material input to the plate interface sediment layer rather than trench sediment at the deformation front (Fig. 2). In the overlying hanging-wall slope basin, sediment strata are tilted in sets of increasing dip with depth, indicating periodic tilting over time from thrusting on the BSFZ fault (Fig. 2). The break in slope is characteristic of active BSFZs.

About 15 km southwest of line 217, line 1235 images a different seismic character (Fig. 3). The BSFZ boundaries are not clearly marked, and the BSFZ appears to be arched over subducted relief at the plate interface. Clarity of the

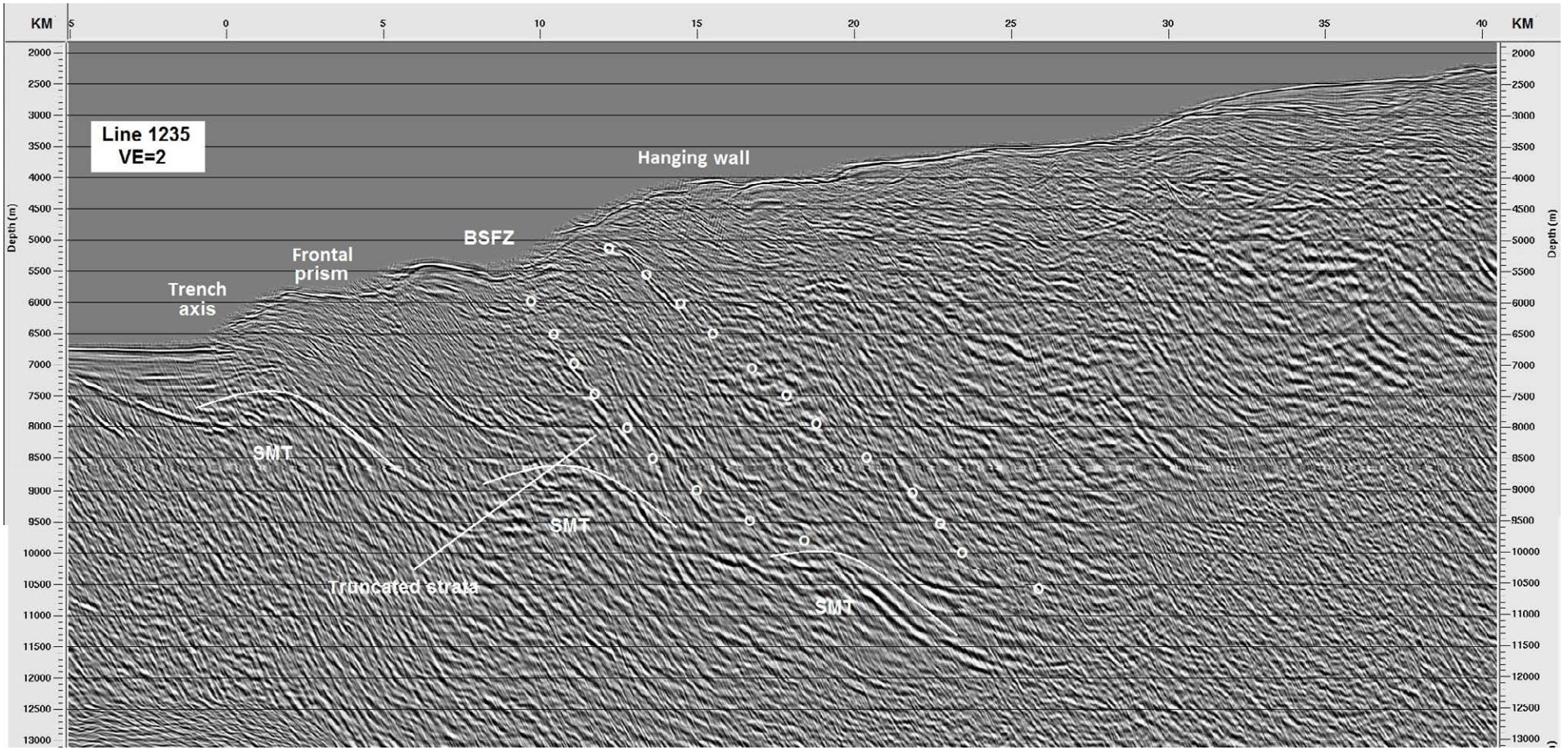

Figure 3. Migrated depth section of legacy line E 1235. Dots approximate the backstop splay fault zone (BSFZ). Clarity of the structure appears degraded by the seismic line's position across the sloping flank of seafloor relief, which hampers two-dimensional imaging. The BSFZ extends to 12 km depth, where its relation to the plate interface sediment layer is concealed by the seafloor multiple. Hanging-wall uplift forms a 1 km step in the seafloor. SMT—seamount or other lower-plate relief. VE—vertical exaggeration.

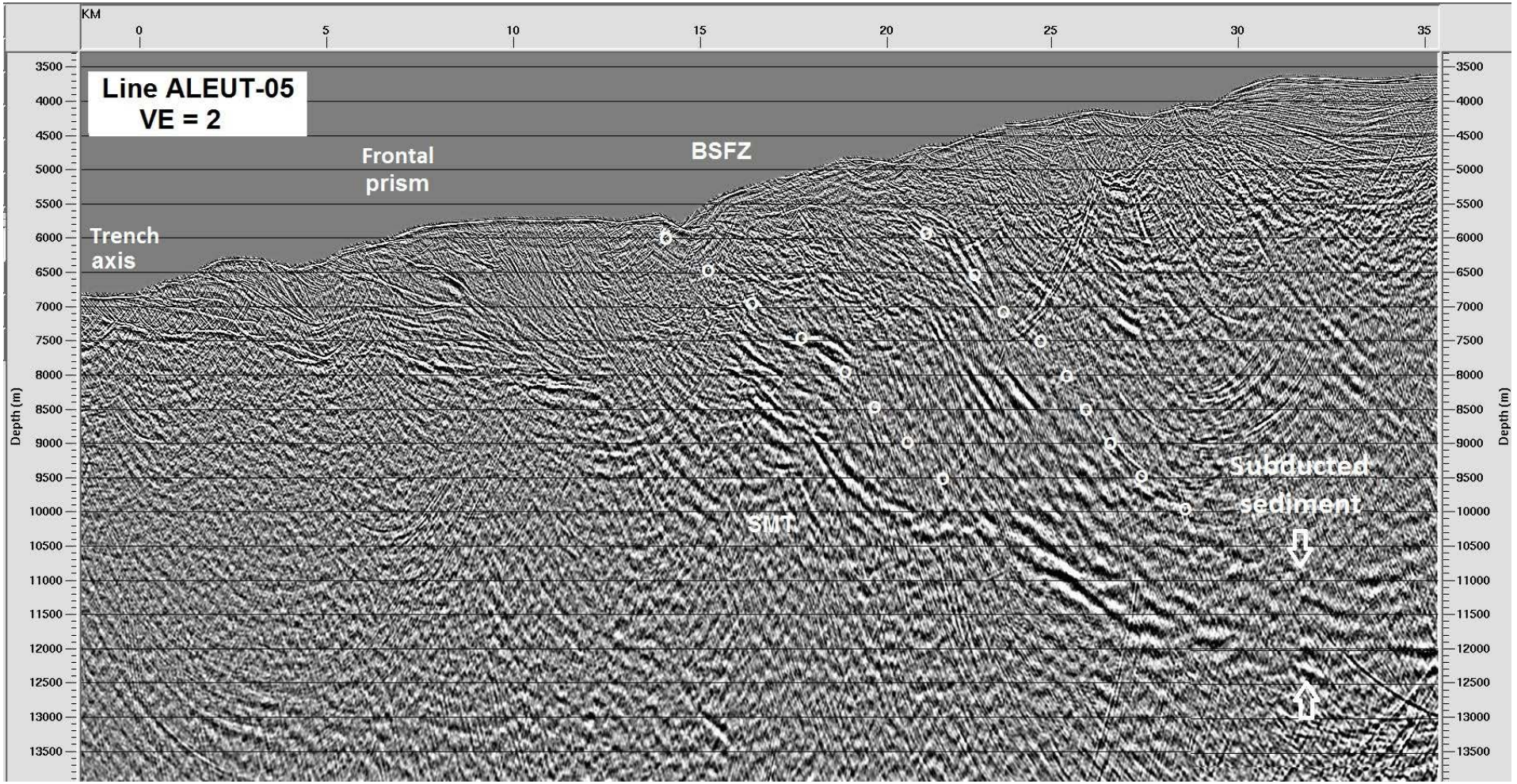

Figure 4. ALEUT line 05 migrated depth section. Landward of the frontal prism this line crosses diagonal trending morphology that parallels the inherited structure of basement (Fig. 1). Backstop splay fault zone (BSFZ) reflections are degraded by the 50° angle between the structural trend and the seismic transect. The upper 1.5 km are complicated by out-of-plane events that may make the thickness appear greater than it is. The footwall boundary is reasonably well marked and the hanging-wall boundary is marked by a strong reflection also imaged by Bécel et al. (2017). No clearly imaged slope basin is perched on the hanging wall, and a mid-slope basin occurs between km 30 and 40. VE—vertical exaggeration; SMT—seamount or other lower-plate relief.

structure may be affected by the seismic line position across the sloping side of seafloor relief, which hampers good two-dimensional imaging. The seafloor multiple obscures structure below a depth of 12 km. Hanging-wall basin strata are irregular (Fig. 3), and below the basin's unconformable floor, the continental framework acoustic basement appears somewhat stratified similar to local simply structured basement outcrops on the Shumagin Islands (Moore, 1972). Hanging-wall uplift is ~800 m, and the fault zone reflectivity is 1.2–1.8 km thick. This unusual thickness may be apparent and result from out-of-plane reflections because structure strikes at an angle to the line of section.

ALEUT line 05 (Fig. 4) crosses the BSFZ amidst small canyons that probably generate side reflections. Strata in the upper 1.5 km of the fault zone have poor coherence (Fig. 4). Below 7 km depth, however, the BSFZ contains strong reflections. The BSFZ appears to locally truncate frontal prism strata. Plate interface reflections with poor coherence beneath the frontal prism at 8–9 km depth may

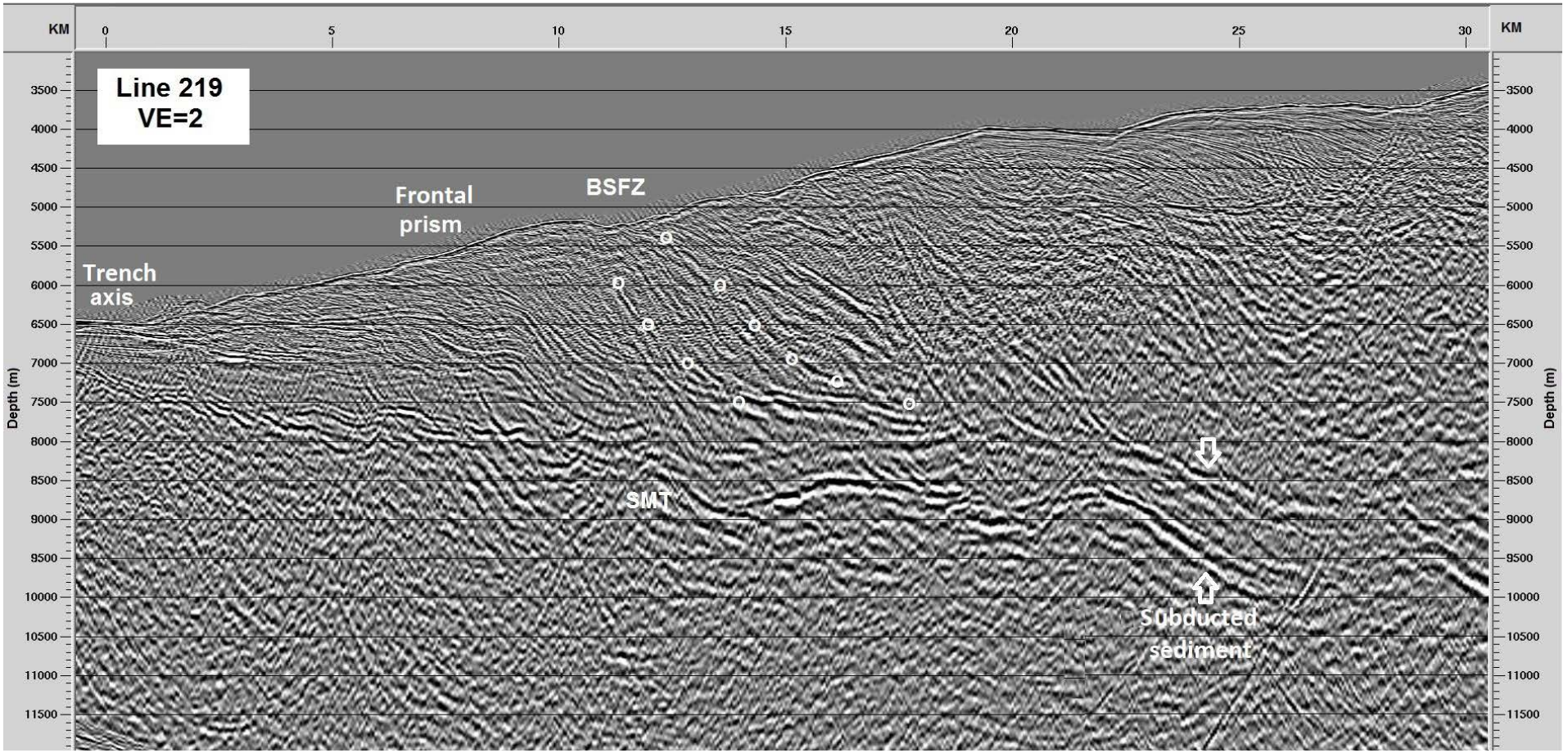

Figure 5. Migrated depth section of legacy line 219. This line crosses the backstop splay fault zone (BSFZ), where its ridge height diminishes (Fig. 1). Outlined with dots is a BSFZ hanging-wall boundary that is the lower one of two that could be a boundary. The upper one could be an en echelon splay fault or a stratified feature in the acoustic basement. VE—vertical exaggeration; SMT—seamount or other lower-plate relief.

indicate lower-plate roughness. The downdip juncture with the plate interface is partly obscured by the seafloor multiple, but weak plate interface reflections and the 1.5-km-thick fault zone of the BSFZ appear to merge. Li et al. (2018) report subduction channel thicknesses 15 km from the trench that are ~200 m less than in our image; those measurements could be more precise than ours because of the more thorough velocity analyses they performed on the channel reflectivity.

Legacy line 219 (Fig. 5) crosses the BSFZ ridge where it is still morphologically obvious but its height has diminished. A modest seafloor notch marks the BSFZ. Its junction with the plate interface is complicated by out-of-plane reflections above the plate interface. Our interpretation of the BSFZ is equivocal. Seaward of the BSFZ and plate interface junction, interface roughness appears to increase with depth in the subduction zone as noted in other images.

ALEUT line 04 (Fig. 6) is located along the SW end of aftershocks from the 1938 Semidi earthquake; these aftershocks mark the end of that rupture segment (Fig. 1). Here, the BSFZ ridge is hardly noticeable in available bathymetric compilations, and the seafloor shows only a low slope break at the BSFZ. The multibeam swath acquired during shooting of the ALEUT seismic transect shows a rough low ridge that ends not far away against a deep canyon. The lower-slope bathymetry also changes immediately to the northeast, where the widening area of accreted prism ridges in the Semidi segment begins.

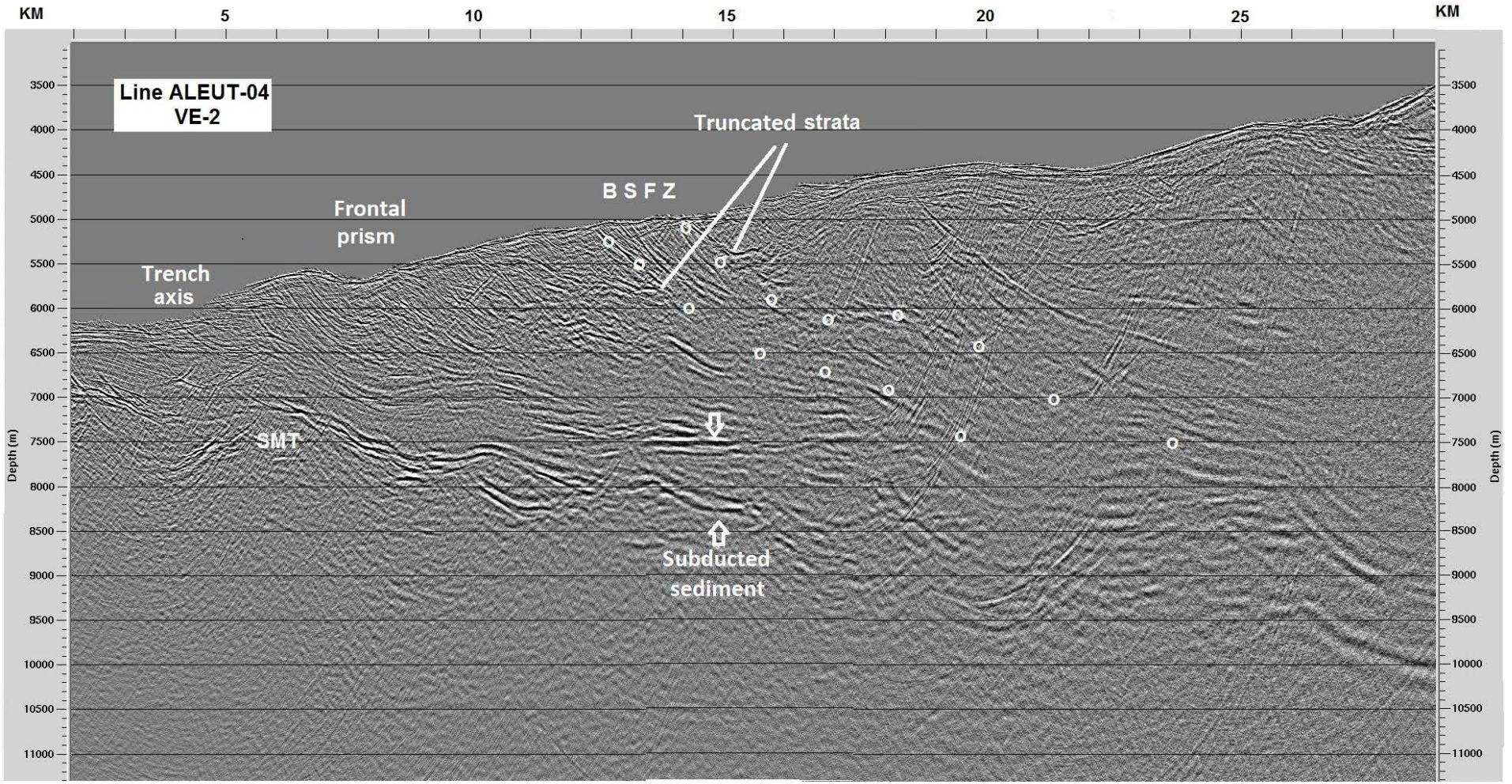

Figure 6. ALEUT line 04 migrated depth section. This image may be typical of the 50-km-long interval NE of line 219 with lack of a clear morphologic ridge until the Semidi segment boundary (Fig. 1). Slope sediment up to 1 km thick covers basement of the margin framework. The BSFZ has little seafloor expression and is interpreted along truncated strata and continuous reflections. Merger of the BSFZ and the plate interface is obscured by the seafloor multiple. A loss of reflection continuity along the plate interface probably indicates rough igneous basement. SMT—seamount or other lower-plate relief; VE—vertical exaggeration.

Upper-Slope Extensional Ridges

The upper-slope extensional fault zone was initially formed at an earlier time represented by strata beneath the slope sediment cover. One age limit can be drawn from the relation of structural trends. The Unimak-Shumagin earthquake segment boundary is formed by the diagonal-trending Sanak Island platform and adjacent basin (Fig. 1). Sanak Island (Moore, 1972) and Sanak Basin (Bruns et al., 1987) strike 40° to the regional trend to the Alaska margin and parallel the Beringian margin (Fig. 1). The long-standing explanation is inheritance from a margin configuration preceding development of the Aleutian arc when the Alaska and Bering margins were joined (cf. Moore, 1972; Bruns et al., 1987; Scholl, 2007). The feature's sizes are substantial in that Sanak Basin is ~170 km long, as deep as 7 km, and the associated insular basement platform is ~40 km wide. These features limited

aftershocks of the 1946 Unimak tsunami earthquake (Lopez and Okal, 2006). The Aleutian arc is a later feature, the trends for which cut across the remnant diagonal Beringian trends. The oldest rocks dredged from the arc have an Early Eocene age (Jicha et al., 2006; Scholl, 2007). The Alaska/Aleutian margin parallel bathymetry includes the upper-slope extensional zone marked by a ridge (Fig. 1). The western part contains the 130-km-long Unimak Ridge on which the ~3-km-high Unimak Seamount erupted. East of the seamount, a less prominent ridge continues the Aleutian/Alaska trend. We refer to this as Shumagin Ridge, and it continues from the indentation northeastward to the Semidi segment boundary (Fig. 1). The 19.8 ± 1.0 Ma age of a sample from Unimak Seamount (Bruns et al., 1987) brackets an initial age of the Unimak and Shumagin ridges as between Early Eocene and Early Miocene.

Seismic Images of Extensional Faults along Shumagin Ridge

Unimak Ridge, shown in the legacy line 205 seismic image, brings basement to a near-surface exposure (Fig. 7). The ridge is formed by an LDE fault that elevated and tilted the basement block. Eocene limestones and shale dredged from the ridge indicate its basement provenance, consistent with its elevated seismic velocity (Bruns et al., 1987). Minimum vertical displacement on the LDE fault is 2.5–3 km, based on dislocation of the Oligocene/Miocene basement unconformity. The LDE fault zone of disrupted reflections is ~2 km wide at its deepest imaged parts. Unimak Seamount age is consistent with the Oligocene–Miocene inferred age of the unconformity flooring the associated basin (Winston, 1983; Bruns et al., 1987; Turner et al., 1987). A flank of Unimak Seamount might be displaced along the LDE fault, as indicated in a

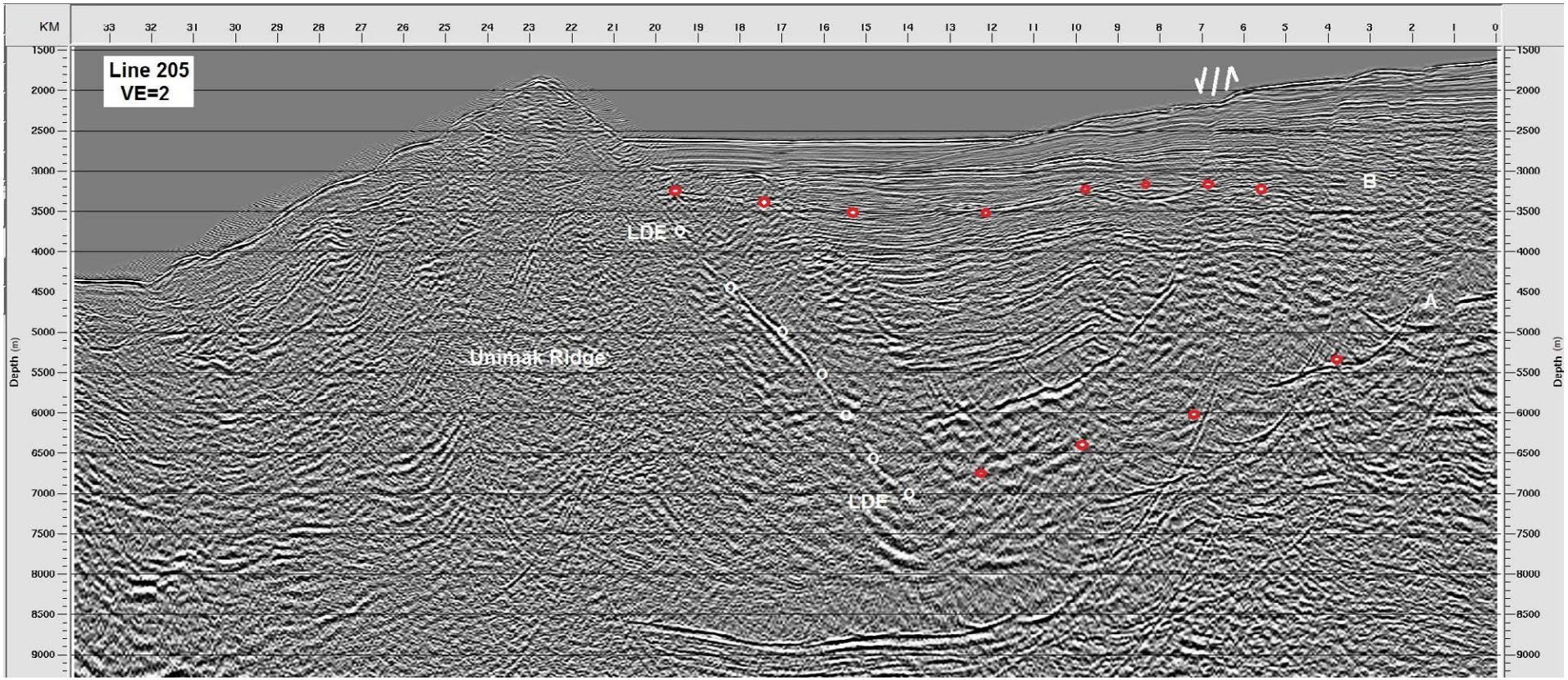

Figure 7. Legacy line 205 depth section crossing western Unimak Ridge. A landward-dipping extensional (LDE) fault forms the half graben basin containing strata whose dip increases with depth indicating growth faulting. Basin-filling strata are cut by landward- and seaward-dipping extensional faults with 100 m to 200 m displacement on lower strata that decreases upward. A and B at red dots approximate dated unconformities indicated by Bruns et al. (1987). Red dots (B) approximate the Late Miocene unconformity; red dots (A) approximate the Oligo-Miocene unconformity on basement. VE—vertical exaggeration.

bathymetric profile acquired during dredging (Bruns et al., 1987). However, displacement on the LDE fault system is inferential because the dredging was performed prior to GPS navigation; so deviation of the ship's course was not recorded.

As mentioned previously, the shelf edge is indented northeast of Unimak Seamount where the Sanak and LDE fault systems intersect. Across that intersection and buried beneath the arched stratal reflections of Shumagin Ridge, legacy line 1235 (Fig. 8) reveals a 4-km-high basement ridge similar to that of Unimak Ridge in line 205 (Fig. 7). The seaward flank of the buried Shumagin Ridge is formed by a seaward-dipping extensional (SDE) fault zone and associated slope basin. The LDE and SDE faults converge beneath the seafloor to form a peak under the morphological Shumagin Ridge. Basin strata dip increases with depth, indicating growth faulting on both flanks. The basin-filling strata are cut by younger and smaller landward- and seaward-dipping normal faults with displacement of only hundreds of meters. About 10 km east of line 1235, legacy line 217 reveals a bifurcation into two 5-km-high ridges flanked by extensional faults (Fig. 9). Weak fault reflections merge at ~10 km depth below the ridges. A fault scarp above the seaward ridge but not the landward one occurs above the LDE and SDE fault convergence. ALEUT line 05 is 15 km farther east (Fig. 10); here, the Shumagin Ridge is broad and only 3 km high, consistent with diminished morphological expression in the overlying bathymetry. Both the LDE and SDE faults are broken along several crossing extensional fractures, some of which run into the overlying basin-filling strata. About 12 km NE of line ALEUT 05, in legacy seismic line 215 (Fig. 11), the

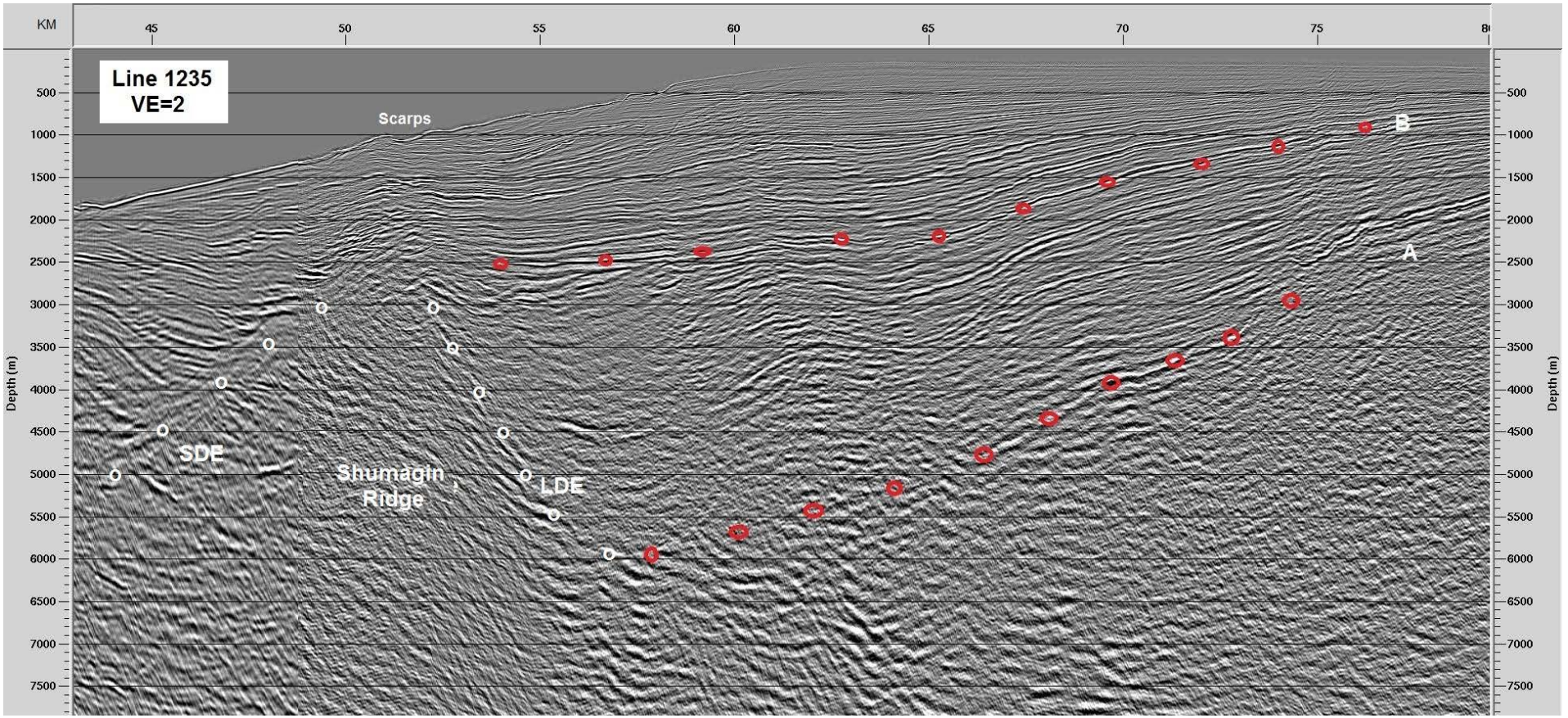

Figure 8. Line 1235, depth section. Red dots (B) approximate the Late Miocene unconformity; red dots (A) approximate the Oligo-Miocene unconformity on basement. Landward-dipping extensional (LDE) and seaward-dipping extensional (SDE) features mark the major extensional faults. The normal faults between km 60 and 65 are typical of many others. Note the seafloor fault scarps above the LDE and SDE intersection. VE—vertical exaggeration.

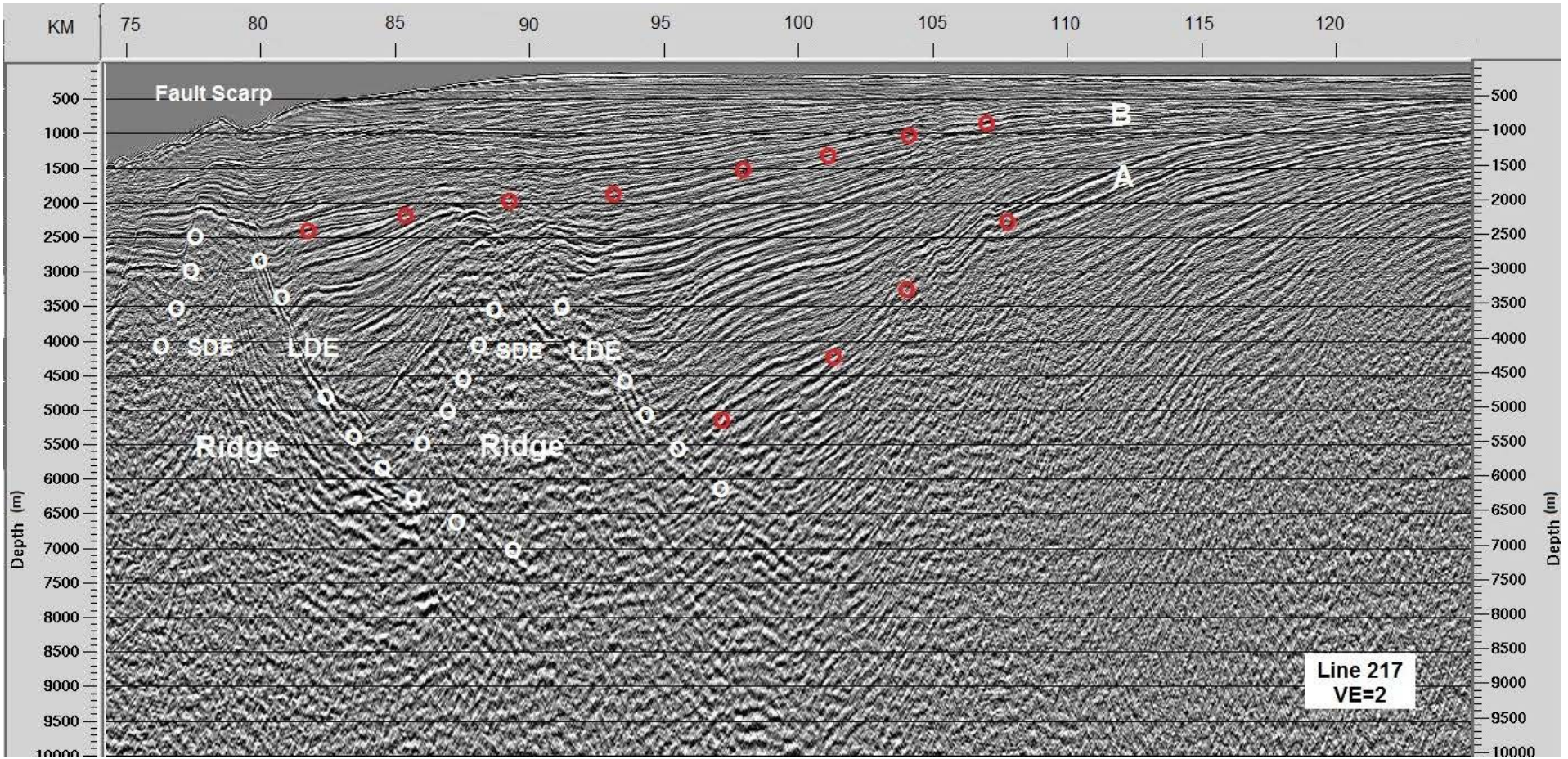

Figure 9. Line 217 depth section showing Shumagin Ridge bifurcation, perhaps an area of en echelon faulted ridges. Seaward ridge has a seafloor scarp, whereas the landward ridge does not. Landward-dipping diffuse reflectivity continues below the basins to the end of the record. LDE—landward-dipping extensional feature; SDE—seaward-dipping extensional feature.

Shumagin basement ridge is only 2–2.5 km high and flanked by the LDE and SDE faults. However, above the basement ridge, the LDE displaces sediment strata and emerges at a small scarp on the seafloor. Line 213 also shows a clear subsurface ridge ~1.5 km high overlain by undeformed strata, but this line is not shown here.

These seismic images show the buried basement structure of an 80-km-long segment of Shumagin Ridge basement that underlies the seafloor ridge in conventional bathymetric maps (Figs. 1 and S3 [footnote 1]). About 60 km farther NE, in the boundary area between the Shumagin and Semidi earthquake segments, line ALEUT 04 (Fig. 12) contains a low basement ridge that is formed by an LDE and SDE of similar displacement. Here, the upper part of the ridge includes the Early Miocene sediment section rather than basement. And rather than an overlying seafloor ridge, the basement ridge is overlain by a basin formed by the opposing half graben on both flanks. Sediment ponding in the basin produces a ~20-km-wide terrace, and strata are only slightly arched at depth above the subsurface ridge.

At the SW end of Shumagin Ridge, ALEUT line 06 (Fig. 13) illustrates structure in the shelf edge indentation at the seaward end of Sanak Basin. It shows a ridge formed by converging LDE and SDE faults, buried beneath ~2-km-thick strata and a 5-km-deep basin upslope. The seafloor scarp indi-

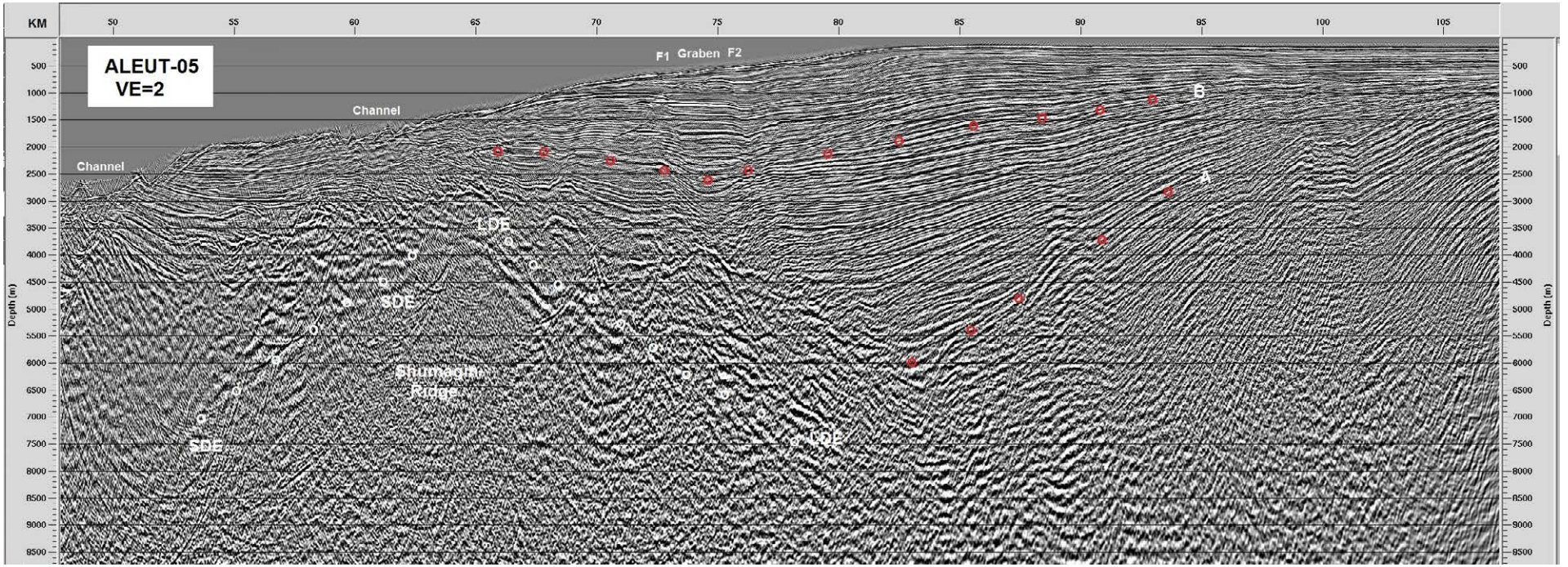

Figure 10. ALEUT line 05 (U.S. Geological Survey processing). The landward-dipping extensional (LDE) fault zone appears modified by short normal faults at 3500–5000 m depth and between km 65 and km 75. Strata in the basin are cut by extensional landward-dipping faults, and F1 and F2 refer to the normal faults annotated in Bécel et al. (2017). The upper slope is incised by channels (Fig. 1). Red dots approximate the Late Miocene and Oligo-Miocene unconformities. VE—vertical exaggeration. SDE—seaward-dipping extensional feature.

cates current faulting above the SDE fault zone. Where the LDE fault zone crosses the Sanak Basin's structural trend, bathymetry is irregular, indicating a disruption of the ridge across the seaward end of Sanak Basin indentation. However, a continuation of Unimak Ridge structure into Shumagin Ridge was probably complicated by the intersection with this major crossing structure.

An unconformity (B in Bruns et al., 1987, their figures 8 and 17) divides the basin sediment along Shumagin Ridge into a lower basin fill and a slope cover. The basin fill is thought to be of Early to Late Miocene age, and the slope cover is Latest Miocene to Quaternary. The inferred age of the upper unconformity allows some estimates of average rates of faulting after ca. 6 Ma based on horizon B vertical displacement.

Within the upper sediment section of line ALEUT 05, annotated extensional growth faults bound either side of a narrow graben (Fig. 10). Unconformity B is displaced 350 +50 m vertically, and across both faults of the graben the unconformity is displaced ~300 m. These graben faults are interpreted to transmit extensional slip traveling from the plate interface to the seafloor, where bathymetry shows a 5-m-high fault scarp (Bécel et al., 2017). Similar grabens occur without a physical connection to an LDE fault zone (Figs. 7–9), and a number of them have similar displacement and seafloor scarps.

DISCUSSION

The implied dynamics of the Shumagin segment set it apart from other Alaska margin segments. Creeping behavior has been suggested to explain the lack of a great earthquake in historic time (Sykes, 1971) and later, strain accumulation, in both standard surveying (Savage et al., 1986) and GPS (Fournier and Freymueller, 2007). However, with only land-based geodetic observations, this inference remains uncertain, and its causes are not understood. Dissimilar tectonic structure might help clarify differences between the Shumagin and adjacent segments, as suggested by Bécel et al. (2017). Geophysical data compiled here show previously unreported tectonic similarities and differences with adjacent segments.

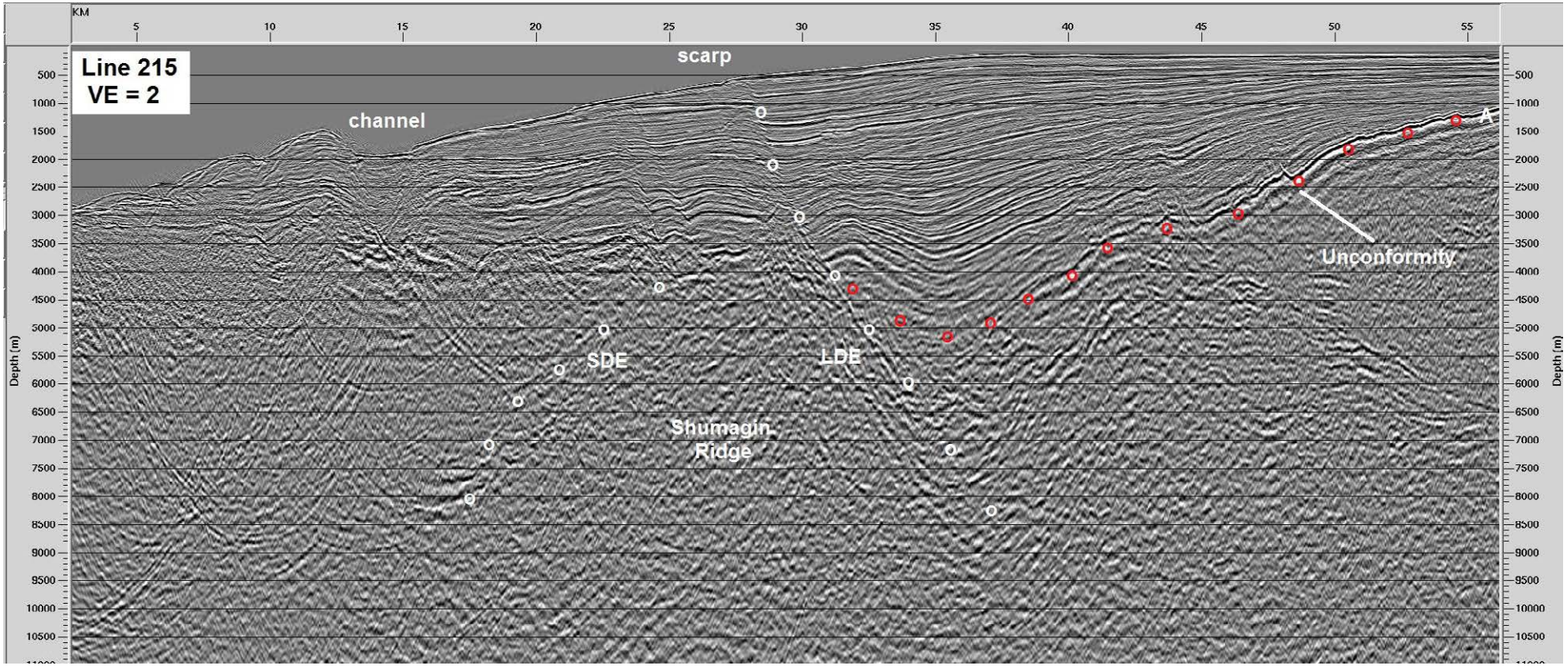

Figure 11. Legacy line 215 depth section. Seafloor scarp marks the exit of the major landward-dipping extensional (LDE) fault. Height of the basement ridge above horizon A is ~2 km less than in ALEUT 05 consistent with the decreased height of the overlying seafloor ridge. Thickness of the upslope basin sediment has also decreased ~1 km. Acoustic basement stratification has increased compared to previous images. VE—vertical exaggeration; SDE—seaward-dipping extensional feature.

A similar feature is the continuous BSFZ along the Shumagin segment observed in seismic images linked with bathymetry (Figs. 1 and 4; Fig. S3 [footnote 1]). The Shumagin BSFZ ridge is less prominent than the Unimak BSFZ ridge, especially in the NE. In the NE, erosional channels are continuous across the BSFZ, whereas in the SW, channels commonly stop at the BSFZ ridge. Evidently, morphological development is more rapid in the SW. BSFZ tectonic activity is inferred from the character of seafloor morphology in the absence of more direct uplift data. Sharp angular relief is considered younger than eroded and rounded bed forms. The sharpest morphology occurs in the SW, whereas to the NE of line 219, the BSFZ ridge becomes almost imperceptible without multibeam bathymetry (Figs. 1 and S4 [footnote 1]). In contrast with seismic lines to the SW, ALEUT 04 has no hanging-wall basin (Fig. 6) that records repeated vertical displacements along the BSFZ (Figs. 2–5). The morphological change from SW to NE is relatively abrupt, and rates of tectonism differ.

A similar trend is observed in the upper-slope fault system. Mid-slope terraces are common to convergent margins, but their underlying structure is not usually as well imaged as in the Shumagin segment upper-slope extensional fault system. Since terraces separate the mid and lower slopes from upper slopes and the shelf, their role as indicators of strain appears significant. The Unimak and Shumagin ridge basement is structured similarly. An LDE fault zone forms Unimak Ridge, and SDE faults are minor (Fig. 7). In the SW Shumagin segment, both LDE and SDE fault zones have a km or more vertical displacements on the basement unconformity (Figs. 8–10 and 13). In the NE, however, the opposing LDE and SDE faults imaged in line ALEUT 04 have much less displacement. Faulted basins filled with sediment form the flat surface of terraces (Figs. 7 and 13) where the rate of sedimentation overwhelms fault displacement. The basement structure seen in ALEUT line 04 is repeated in the SW Shumagin segment, but with greater fault displacement relative to sedi-

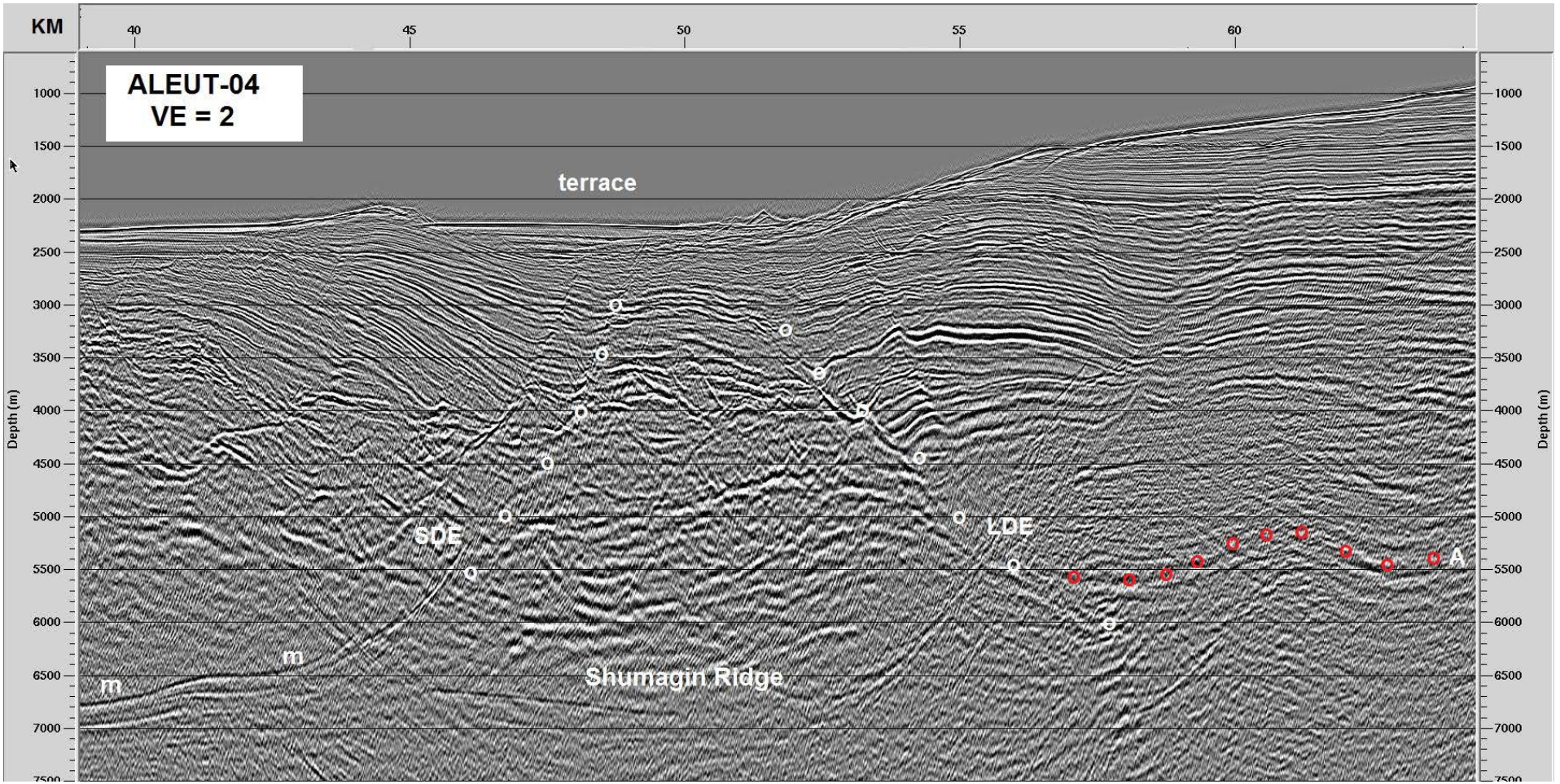

Figure 12. ALEUT 04 depth section (U.S. Geological Survey processing). The continuation of Shumagin Ridge to this location is inferred from morphology. Horizon B was not identified with confidence M—multiple. Minor extensional faults cut the slope cover. VE—vertical exaggeration; LDE—landward-dipping extensional feature; SDE—seaward-dipping extensional feature.

mentation. Here, rather than a terrace over the basement high, a ridge runs along the SW part of the segment—despite no indications of a great change in rate of sedimentation. Rates of fault zone displacement appear to have been greater in the SW than in the NE halves of the Shumagin segment.

The abrupt decline of morphological expression in both the upper-slope extensional zone and the BSFZ suggests a common tectonic system (Figs. 14 and S4 [footnote 1]). Upper-slope extension appears compensated by BSFZ or frontal prism contraction. Bécel et al. (2017) mention a similar tectonic scheme.

A Unimak segment tsunami investigation included a diagram relating movement in the mid-slope area of extension to thrusting on the BSFZ (von Huene et al., 2016). With a few modifications, the diagram is relevant to the Shumagin segment (Fig. 14). An important implication of both diagrams is an apparent mechanical isolation of the upper-plate wedge seaward of the mid-slope extensional area. How does the strain monitored geodetically on land differ from strain across the continental slope wedge? Despite being separated by a zone of major extension, the upper and middle slope also display many small normal faults (Figs. 9–13). Contractile deformation begins in proximity

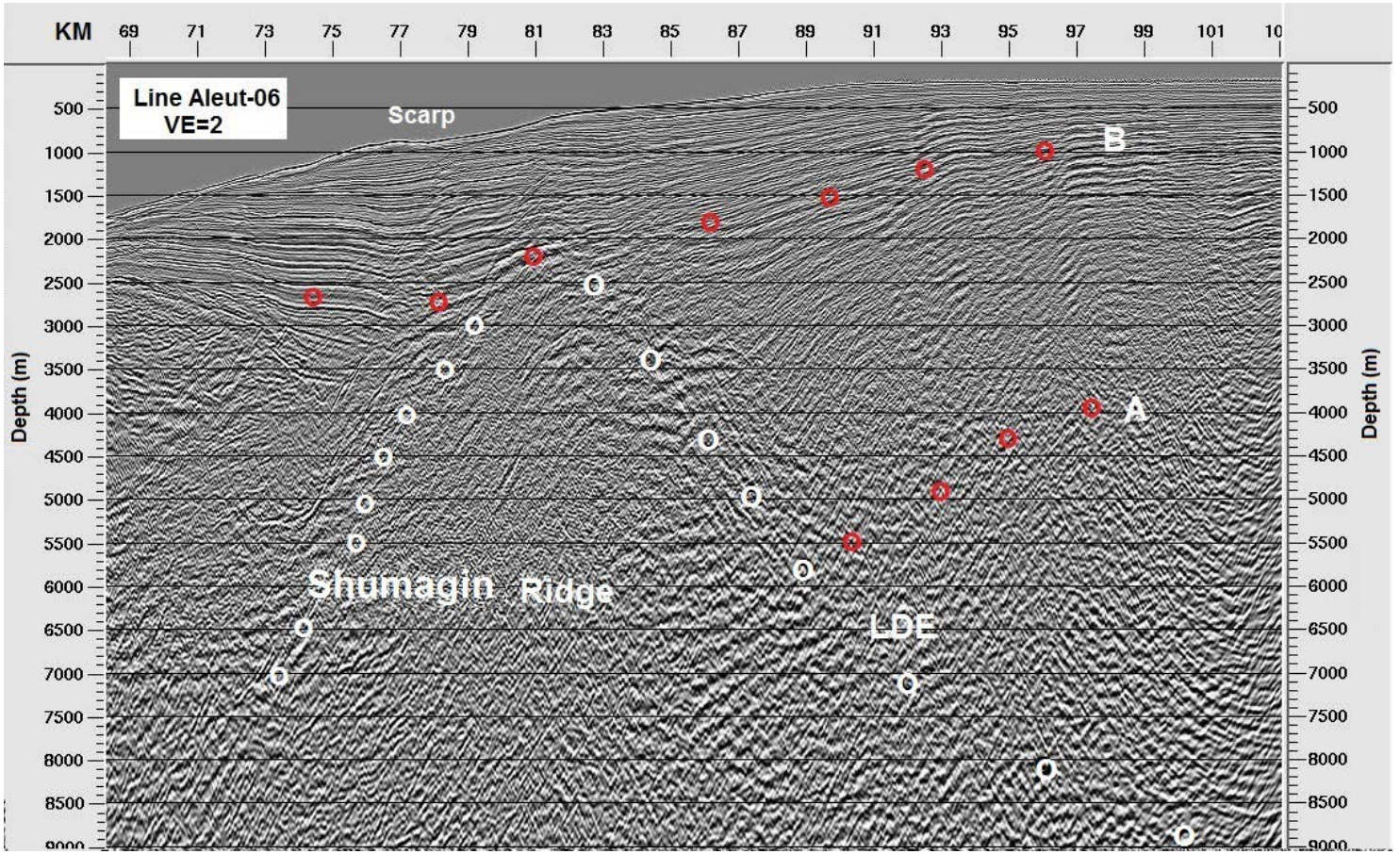

Figure 13. ALEUT 06 depth section (U.S. Geological Survey processing). This transect is located in the indentation where Unimak Ridge faults cut the seaward end of Central Sanak Basin and faults. Dots approximate the landward-dipping extensional (LDE) fault zone; upper and lower red dots approximate the Late Miocene and the Oligocene/Miocene unconformity on basement. Minor extensional faults cut the slope cover. VE—vertical exaggeration.

to the BSFZ. Regardless of separation from the upper slope, the mid-slope block is strong enough to stand firm against contractile deformation during the earthquake cycle. Its rigidity may be similar to that of the upper slope and shelf and significantly more than that of the frontal prism.

Against this background of mostly similar features, what are some differences? Tectonic dissimilarity between the Shumagin and other segments builds on the former connection of the Alaska and Bering margins and their separation during Aleutian Arc development. In the scenario for the origin of the Aleutian–Bering Sea region of Scholl (2007), this happens between 50 and 55 Ma. The diagonal Sanak tectonic zone derives its tectonic trend from a position at the locus of arc capture when the Bering-Alaska juncture was disrupted to become the Alaska-Aleutian arc (cf. summary of Scholl, 2007, and citations therein). If Bering and/or Alaska structural trends survived, one could question whether Bering basement also underlies the Shumagin segment. In bathymetric maps, the current Shumagin shelf edge projects ~20 km farther seaward than adjacent segments (Fig. 1), which is consistent with a greater seaward extension of basement. The location of the outer Shumagin Islands in proximity to the shelf edge is consistent with shallow basement near the shelf edge (Figs. 7–10) and with positive free-air gravity anomalies (Sandwell and Smith, 1997).

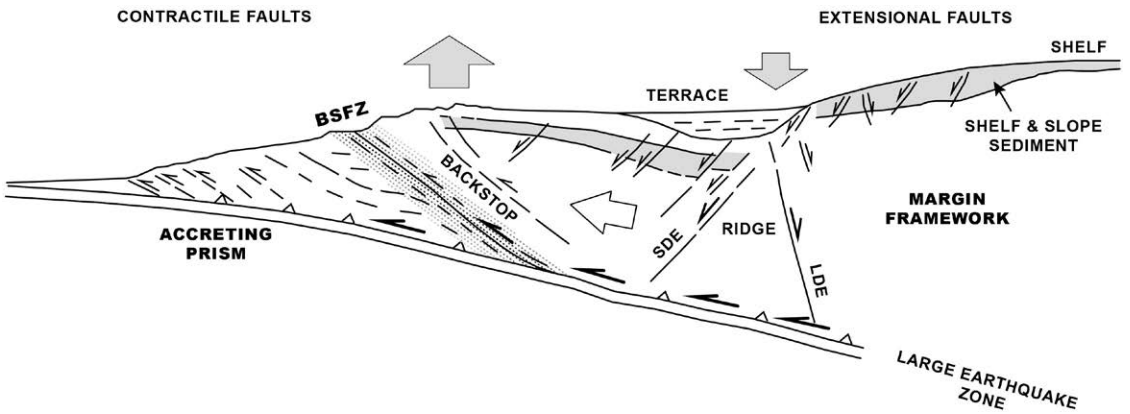

Figure 14. Diagram of the interaction between Shumagin Ridge extension and the backstop splay fault zone (BSFZ). Abbreviations: SDE—seaward-dipping extensional fault; LDE—landward-dipping extensional fault.

The plate interface dip depicted in Slab 1.0 (Hayes et al., 2012) varies from shallow beneath the Sanak Island platform to steeper opposite the Shumagin Islands and then shallower again northeast of the islands. Refraction seismic transects across the Unimak (Lizarralde et al., 2002) and Kodiak segments image a plate interface dip that is ~6 m shallower than that of ALEUT line 05 across the Shumagin segment (Bécel et al., 2017). The agreement between dips in refraction transects and Slab 1.0 lends confidence in Slab 1.0 deviation around the Shumagin Islands.

The unusually narrow frontal prism noted by Bécel et al. (2017) is typical of the Shumagin segment. The width of frontal prism segments undisturbed by subduction of lower-plate relief averaged ~20 km in the Kodiak segment, 24 km in the Semidi segment, 13 km in the Unimak segment, and only 10 km in the Shumagin segment. The difference in width is difficult to attribute to an unusual character of the incoming ocean crust or volume of trench sediment. GLORIA sidescan images show no major relief in the ocean basin, and they show uniform development of bend faults at an angle to the deformation front. However, in the subduction zone, the plate interface images contain considerable subducting relief that is ~2 km high. Subducting relief beneath the frontal prism is puzzling considering the lack of any seafloor relief on the incoming plate. Bend faulting of the lower plate after subduction is a possible explanation. The effects of variable subducting sediment thicknesses along the plate interface have recently been studied by Li et al. (2018). They relate the effect of sediment thickness on pore pressure that may be linked to fault behavior.

These indications of a distinctive geology do not yet offer an obvious explanation for the Shumagin gap's creeping behavior. The Shumagin segment's geology differs from other segments, but a link to its seismic behavior is beyond the resolution of available data. Marine geodetic observations may show whether the seaward part of the margin framework is detached from the landward part. Whether mid-slope extensional structures root in the plate interface (Bécel et al., 2017) is not likely to be determined without RV *Langseth*–type seismic acquisition capabilities. Seafloor geodesy would be a major contributor to assessment of earthquake hazards.

A key aspect of Shumagin segment geology applicable to other convergent margins is recognition of significant extensional tectonism landward of the lower slope. Extensional structure is more common than has been appreciated in much of the literature. Well-developed mid-slope terraces can be extensional structures. Terraces are commonly more obvious in a margin's morphology than the ridge formed by an active BSFZ. Along the Shumagin and Unimak margins, extensional structure is not as deeply buried or perhaps as complex as on many other margins, and thus they can serve as a model to consider where conditions obscure deep structure in seismic data.

SUMMARY AND CONCLUSIONS

We integrated reprocessed legacy and more recent seismic data with bathymetry—both multibeam and conventional—and GLORIA images in the Shumagin earthquake segment. Developments in understanding of convergent margin tectonics and the advancement of analytical systems since a first report in 1985 (Bruns et al., 1985) allowed resolution of unreported tectonic features. An Alaskan backstop splay fault zone (BSFZ) extends along the Shumagin margin, filling a gap between BSFZs in adjacent earthquake segments. The BSFZ hanging-wall morphology indicates recent activity in the SW. Morphology bridges a diverse structure observed in seismic images. The SW half of the segment has a rough morphology, whereas the NE half displays a smoother morphology consistent with decreased tectonic deformation in subsurface information. Rates of tectonism differ in two parts of the segment.

In seismic images, the BSFZ fault zone consists of disrupted reflections in a damage zone. Where the BSFZ extends into the plate interface, its reflections cut across much of the subducted sediment strata and merge into it. The BSFZ

damage zone could be a source of clastic material input to plate-interface subducted sediment. When the BSFZ is active, slip beneath the frontal prism is diminished. Alternatively, with the BSFZ truncated at the plate interface, slip may propagate to the deformation front. BSFZ activity appears to be linked with subducting relief.

Along the upper slope, a low ridge underlain by an extensional fault zone is similar to a ridge seen in the Unimak segment. Informally named Shumagin Ridge, it forms a 3–4-km-deep sediment-filled basin. Its subsurface and seafloor expression declines in the NE half of the segment, as does the BSFZ. Much of the extensional fault displacement may have occurred prior to 20 m.y. ago, as in the Unimak segment.

Slope sediment dating from Latest Miocene to Holocene covers Shumagin Ridge and is cut by many extensional growth faults. Their vertical displacement is relatively small and usually does not exceed 400 m. Some of these faults connect with Shumagin Ridge LDE and SDE faults. Activity on the connected normal faults can be explained by continued displacement on the basement faults and downslope gravity extensional forces.

The Shumagin Ridge causative faults displace the regional Oligocene/Miocene unconformity. Unimak Seamount's 20 Ma age provides a probable youngest age, thereby bracketing the extensional fault origin as between Oligocene and earliest Miocene. Interaction between the extensional fault system and the BSFZ appears likely. The Shumagin BSFZ, like those in adjacent segments, is a potential tsunami generator.

ACKNOWLEDGMENTS

We benefited from discussions with David Scholl and thank Peter Dartnell, U.S. Geological Survey (USGS), for illustrations from his previous bathymetric compilations. Greg Moore shared a Nankai splay fault image for comparison with line 217. Reviews by Maureen Walton and Ginger Barth of the USGS, an anonymous journal reviewer, Donna Shillington, and guest editor Laura Wallace were essential in improving earlier versions of this report. RvH received support for travel from Menlo Park to Denver from a USGS emeritus scientist support fund. The assistance and patience of Gina Harlow and GSA staff throughout the evolution of this contribution is greatly appreciated.

REFERENCES CITED

Bécel, A., Shillington, D.J., Delescluse, M., Nedimović, M.R., Abers, G.A., Saffer, D.M., Webb, S.C., Keranen, K.M., Roche, P.-H., Li, J., and Kuehn, H., 2017, Tsunamigenic structures in a creeping section of the Alaska subduction zone: Nature Geoscience, v. 10, p. 609–613, https://doi.org/10.1038/ngeo2990.

Bruns, T.R., von Huene, R.E., Culotta, R.C., and Lewis, S.D., 1985, Summary geologic report for the Shumagin Outer Continental Shelf (OCS) planning area, Alaska: U.S. Geological Survey Open-File Report 85-32, 58 p., https://doi.org/10.3133/ofr8532.

Bruns, T.R., von Huene, R., and Culotta, R.C., 1987, Geology and petroleum potential of the Shumagin margin, Alaska, *in* Scholl, D.W., Grantz, A., and Vedder, J.G., eds., Geology and Resource Potential of the Continental Margin of Western North America and Adjacent Ocean Basins—Beaufort Sea to Baja California: Houston, Texas, Circum-Pacific Council for Energy and Mineral Resources, Earth Science Series, v. 6, p. 157–190.

Burk, C.A., 1965, Geology of the Alaska Peninsula—Island Arc and Continental Margin (Part 1): Geological Society of America Memoir 99, 250 p.

Fournier, T.J., and Freymueller, J.T., 2007, Transition from locked to creeping subduction in the Shumagin region, Alaska: Geophysical Research Letters, v. 34, L06303, https://doi.org/10.1029/2006GL029073.

Hayes, G.P., Wald, D.J., and Johnson, R.L., 2012, Slab1.0: A three-dimensional model of global subduction zone geometries: Journal of Geophysical Research, v. 117, B01302, https://doi.org/10.1029/2011JB008524.

Jicha, B.R., Scholl, D.W., Singer, B.S., Yogodzinski, G.M., and Kay, S.M., 2006, Revised age of Aleutian Island Arc formation implies high rate of magma production: Geology, v. 34, no. 8, p. 661–666, https://doi.org/10.1130/G22433.1.

Kanamori, H., 1972, Mechanism of tsunami earthquakes: Physics of the Earth and Planetary Interiors, v. 6, p. 346–359, https://doi.org/10.1016/0031-9201(72)90058-1.

Lewis, K.B., Ladd, J.W., and Bruns, T.R., 1988, Structural development of an accretionary prism by thrust and strike-slip faulting, Shumagin region, Aleutian Trench: Geological Society of America Bulletin, v. 100, p. 767–782, https://doi.org/10.1130/0016-7606(1988)100<0767:SDOAAP>2.3.CO;2.

Li, J., Shillington, D.J., Becel, A., Nedimovic, M.R., Webb, S.C., Saffer, D.M., Keranen, K.M., and Kuehn, H., 2015, Downdip variations in seismic reflection character: Implications for fault structure and seismogenic behavior in the Alaska subduction zone: Journal of Geophysical Research, v. 120, p. 7883–7904, https://doi.org/10.1002/2015JB012338.

Li, J., Shillington, D.J., Saffer, D.M., Becel, A., Nedimovic, M.R., Kuehn, H., Webb, S.C., Keranien, K.M., and Abers, G.A., 2018, Connections between subducted sediment pore-fluid pressure and earthquake behavior along the Alaska megathrust: Geology, https://doi.org/10.1130/G39557.1.

Liberty, L.M., Finn, S.P., Haeussler, P.J., Pratt, T.L., and Peterson, A., 2013, Megathrust splay faults at the focus of the Prince William Sound asperity: Journal of Geophysical Research, v. 118, p. 1–14, http://onlinelibrary.wiley.com/doi/10.1002/jgrb.50372/abstract.

Lim, E., Eakins, B.W., and Wigley, R., 2009, Coastal Relief Model of Southern Alaska: Procedures, Data Sources and Analysis: NOAA Technical Memorandum NESDIS NGDC-43, 22 p., http://www.ngdc.noaa.gov/mgg/coastal/s_alaska.html.

Lizarralde, D., Holbrook, W.S., McGeary, S., Bangs, N.L., and Diebold, J.B., 2002, Crustal construction of a volcanic arc, wide-angle seismic results from the western Alaska Peninsula: Journal of Geophysical Research: Solid Earth, v. 107, no. B8, p. EPM 4-1–EPM 4-21, https://doi.org/10.1029/2001JB000230.

Lopez, A. M., and Okal, E. A., 2006, A seismological reassessment of the source of the 1946 Aleutian 'tsunami' earthquake: Geophysical Journal International, v. 165, no. 3, p. 835–849.

Miller, J.J., von Huene, R., and Ryan, H.F., 2014, The 1946 Unimak Tsunami Earthquake Area: Revised tectonic structure in reprocessed seismic images and a suspect near field tsunami source: U.S. Geological Survey Open-File Report 2014-1024, 19 p., https://doi.org/10.3133/ofr20141024.

Moore, G.F., Bangs, N.L., Taira, A., Kuramoto, S., Pangborn, E., and Tobin, H.J., 2007, Three-dimensional splay fault geometry and implications for tsunami generation: Science, v. 318, p. 1128, https://doi.org/10.1126/science.1147195.

Moore, J.C., 1972, Uplifted Trench Sediments: Southwestern Alaska-Bering Shelf edge: Science, v. 175, no. 4026, p. 1103–1105, https://doi.org/10.1126/science.175.4026.1103.

Paskevich, V.F., Wong, F.L., O'Malley, J.J., Stevenson, A.J., Gutmacher, C.E., 2010, GLORIA sidescan-sonar imagery for parts of the U.S. Exclusive Economic Zone and adjacent areas: U.S. Geological Survey, Open-File Report 2010-1332.

Sandwell, D.T., and Smith, W.H.F., 1997, Marine gravity anomaly from Geosat and ERS satellite altimetry: Journal of Geophysical Research, v. 102, B5, p. 10,039–10,054, https://doi.org/10.1029/96JB03223.

Savage, J.C., Lisowski, M., and Prescott, W.H., 1986, Strain accumulation in the Shumagin and Yakataga seismic gaps, Alaska: Science, v. 231, p. 585–587, https://doi.org/10.1126/science.231.4738.585.

Scholl, D.W., 2007, Viewing the Tectonic Evolution of The Kamchatka-Aleutian (KAT) Connection with an Alaska Crustal Extrusion Perspective, *in* Eichelberger, J., Gordeev, E., Izbekov, P., Kasahara, M., and Lees, J., eds., Volcanism and Subduction: The Kamchatka Region: American Geophysical Union, Geophysical Monograph Series 172, https://doi.org/10.1029/172GM03.

Sykes, L.R., 1971, Aftershock zones of great earthquakes, seismicity gaps, and earthquake prediction for Alaska and the Aleutians: Journal of Geophysical Research, v. 76, p. 8021–8041, https://doi.org/10.1029/JB076i032p08021.

Turner, R.F., Lynch, M.B., Conner, T.A., Halin, P.J., Hoose, P.I., Martin, G.C., Olson, D.L., Larson, J.A., Fett, T.O., Sherwood, K.W., and Adams, A.J., 1987, Geological and operational summary, Kodiak Shelf stratigraphic test wells, Alaska: U.S. Department of the Interior, U.S. Minerals Management Service (MMS), Alaska, USA OCS Report MMS87-862 0109, 341 p.

von Huene, R., Fisher, M.A., and Bruns, T.R., 1987, Geology and evolution of the Kodiak margin, Gulf of Alaska, *in* Scholl, D.W., Grantz, A., and Vedder, J.G., eds., Geology and Resource Potential of the Continental Margin of Western North America and Adjacent Ocean Basins—Beaufort Sea to Baja California: Houston, Texas, Circum-Pacific Council for Energy and Mineral Resources, Earth Science Series, v. 6, p. 191–212.

von Huene, R., Kirby, S., Miller, J., and Dartnell, P., 2014, The destructive 1946 Unimak near-field tsunami: New evidence for a submarine slide source from reprocessed marine geophysical data: Geophysical Research Letters, v. 41, p. 6811, https://doi.org/10.1002/2014GL061759.

von Huene, R., Miller, J.J., Klaeschen, D., and Dartnell, P., 2016, A possible source mechanism of the 1946 Unimak Alaska Far-Field Tsunami: Uplift of the mid-slope terrace above a splay fault zone: Pure and Applied Geophysics, https://doi.org/10.1007/s00024-016-1393-x.

Wendt, J., Oglesby, D.D., and Geist, E.L., 2009, Tsunamis and splay fault dynamics: Geophysical Research Letters, v. 36, L15303, https://doi.org/10.1029/2009GL038295.

Winston, J.G., 1983, Kodiak Shelf, Gulf of Alaska: American Association of Petroleum Geology, Studies in Geology, v. 15, no. 3, p. 140–146.